

A reliable externally fixated murine femoral fracture model that accounts for variation in movement between animals

Chris K. Connolly^a, Gang Li^{a,*}, Jonathan R. Bunn^a, Moses Mushipe^a,
Glenn R. Dickson^b, David R. Marsh^a

^a Trauma Research Group, Department of Trauma and Orthopaedic Surgery, Queen's University Belfast, Musgrave Park Hospital, Belfast, BT9 7JB, Northern Ireland, UK

^b Department of Anatomy, Medical Biology Centre, 97 Lisburn Road, Belfast, BT9 7BL, UK

Received 21 October 2002; accepted 31 January 2003

Abstract

Fifty-two CFLP mice had an open femoral diaphyseal osteotomy held in compression by a four-pin external fixator. The movement of 34 of the mice in their cages was quantified before and after operation, until sacrifice at 4, 8, 16 or 24 days. Thirty-three specimens underwent histomorphometric analysis and 19 specimens underwent torsional stiffness measurement. The expected combination of intramembranous and endochondral bone formation was observed, and the model was shown to be reliable in that variation in the histological parameters of healing was small between animals at the same time point, compared to the variation between time-points. There was surprisingly large individual variation in the amount of animal movement about the cage, which correlated with both histomorphometric and mechanical measures of healing. Animals that moved more had larger external calluses containing more cartilage and demonstrated lower torsional stiffness at the same time point. Assuming that movement of the whole animal predicts, at least to some extent, movement at the fracture site, this correlation is what would be expected in a model that involves similar processes to those in human fracture healing. Models such as this, employed to determine the effect of experimental interventions, will yield more information if the natural variation in animal motion is measured and included in the analysis. © 2003 Orthopaedic Research Society. Published by Elsevier Ltd. All rights reserved.

Keywords: Fracture healing; Animal movement; External fixation; Histomorphometry; Mechanical testing; Mouse

Introduction

A fracture model is a system employed to study fracture healing, of relevance to human fracture healing as encountered in medical practice. The most representative (valid) model would therefore be a human fracture; however, the high validity of a human fracture model must be balanced against poor reliability due to extensive variation between cases in clinical practice. At the opposite extreme, cell culture models are much more reliable but are deficient in validity as a representation of the whole fracture healing process. Between these extremes lie models in various species and sizes of animal, which offer the possibility of adequate numbers of reasonably similar cases of fracture healing occurring in

a whole-organism context, in other words, a balance between reliability and validity.

The criterion of reliability used was a measure of the reproducibility of the rate of fracture healing: that the variation in parameters of healing between animals at each time point should be small in comparison to that observed between time points. The criteria of validity used were that the mode of healing should be recognisable as that displayed in the clinical setting and that the healing should respond to variation in mechanical stimulation in a similar way to human fractures.

Model reproducibility is essential for valid investigation and comparison of fracture healing. Several small and large animal models are reported for the investigation of fracture repair in the mouse [11], rat [4,9,17], rabbit [1], sheep [5,6], dog [22] and goat [20]. All include variation of important influences on bone repair such as the nature of the fracture, its stability, mechanical stress environment, the fixation device applied and success of fracture reduction. Small animals such as the mouse are

* Corresponding author. Tel.: +44-2890-669501x2830; fax: +44-2890-661112.

E-mail address: g.li@qub.ac.uk (G. Li).

attractive candidates for investigating bone healing, particularly for studies focused on molecular questions, because of the availability of gene knockouts, antibodies and gene probes [15]. Studies that address biomechanical aspects of fracture healing tend, with few exceptions [11,16] to be presumed to require larger animal models, and the issue of the biomechanical environment in the small-animal models is tacitly assumed to be irrelevant. The current study challenges that assumption. It aims to show that, in a reliable and valid murine fracture model, the mechanical environment differs between animals due to natural variation in their locomotor behaviour and that this variation influences fracture healing.

Materials and methods

An externally fixated murine femoral osteotomy model was modified from that developed initially by Andrews's group of University of Manchester, UK [10,14]. A whole-animal motion quantification system was developed to provide an index of the loading being experienced by the healing osteotomy. The outcome measures were animal motion in 34 animals, histomorphometry, in a group of animals sacrificed at days 4, 8, 16 and 24 from operation, and torsional stiffness, in a group sacrificed at day 16.

Surgical procedure

Fifty-two male, 3 month old CFLP (Carworth Farms Lane-Petter) mice (Laboratory Services, Queen's University of Belfast) were weighed, anaesthetised and had their left hindquarter shorn. General anaesthesia consisted of 2% Isoflurane (Abbott Laboratories Ltd., Queensborough, Kent, UK) in a 50:50 mixture of N₂O₂:O₂ (BOC N. Ireland Plc., UK) via a Hunt mask, 2 l/min, with a scavenging system. A bolus of 1 ml of 5% dextrose was given subcutaneously at induction for fluid replacement. The femoral shaft was clamped in a drilling jig, shown schematically in Fig. 1A, used to drill five holes. The middle hole was used to weaken the bone at the site of osteotomy. On each of the proximal and distal fragments, a pair of 0.55 mm diameter drill holes were angled as shown in Fig. 1A, each at 7° to the perpendicular, in order to resist pullout. The fixator pins consisted of a core of 0.4 mm steel wire, wound round with nickel filament to an external diameter of 0.55 mm, with a sleeve, consisting of a section of 16-gauge hypodermic needle, over the pins external to the bone. After their insertion, the fixator bar was applied loosely, prior to performing a low energy transverse osteotomy at the site of the central perpendicular drill hole.

The distance between the proximal and distal holes in the fixator bar was 200 µm less than the corresponding distance in the drilling jig. Therefore, sliding the fixator bar down the pins produced compression of the fracture fragments. A 4 mm reduction block ensured replication of the fixator offset. Crimping the pins and sleeves above the crossbar and gluing with polymethacrylate secured the external fixator (Fig. 1B). The animal was then recovered for 5 min under a heat lamp prior to being placed in the cage.

Motion analysis

Thirty-four of the mice had motion analysis performed, of which 3 were sacrificed on day 4, 4 on day 8, 23 on day 16 (including the 19 animals whose fractures were mechanically assessed) and 4 on day 24.

Animal motion was quantified by an infrared (IR) beam detection system fitted to each cage. The IR system operated at a wavelength of 890 nm and consisted of IR diodes and detectors (RS Components, UK), each pair being 130 mm apart across the width of the cage. Each cage was spanned by three parallel beams, at a height of 35 mm from the cage floor and 100 mm apart, with the first and last beams being 50 mm from the ends of the cage. When a beam was broken, a count registered on an electronic counter (RS Components, UK) and a further count registered only when an adjacent beam was broken, so that

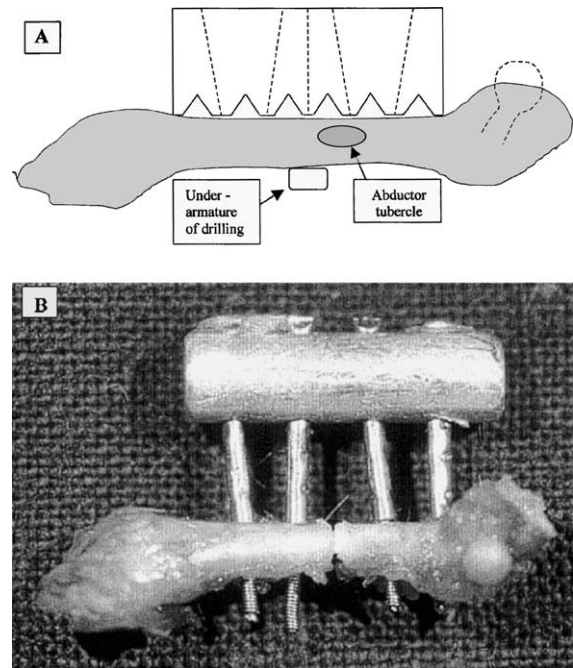


Fig. 1. (A) Line diagram demonstrating the drilling jig position on a left femur and (B) medial view of externally fixated femur with soft tissues removed.

neither head nor tail movements registered a count. Counts were registered continuously over 24-h periods and converted to mean hourly movements for each animal.

Factors previously noted to affect the animal motion profiles were noise, changing the animal's bedding, the light and dark cycle and the ambient room temperature. Housing the 12 motion detectors in an isolated windowless, thermostatically controlled room with an 8 am to 8 pm light cycle minimised these factors. The bedding was never changed but filtered of excrement, on day 17, so as not to remove the animal's scent; this had previously been observed to markedly increase animal motion. The room was only entered to perform the motion readings.

X-ray analysis

Prior to sacrifice the mice were anaesthetised as above and killed by intra-cardiac aspiration of blood at 4, 8, 16 and 24 days post-fracture. The left thigh was excised by sharp dissection disarticulation through the knee and hip joints with the external fixator and soft tissues in situ, thus preventing disruption of the fracture callus and the fracture fragment alignment. The specimen was immediately labelled and tissue fixation commenced at this point. Two orthogonal oblique radiographs (Fig. 2) were taken of each specimen employing a positioning jig, which used the external fixator crossbar as the axis through which the specimen was rotated through 90°. The radiographs were magnified 11×, onto a screen to reduce measurement error. Contact (the percentage of the fracture surfaces in contact) and alignment of the fragments were measured in each view. Since the fracture was held in compression, there was no fracture gap visible.

Tissue preparation and histomorphometry

Specimens were coded and fixed in 10% buffered formalin, decalcified in 8% EDTA, dehydrated in ethanol and embedded in paraffin wax. The external fixators were removed from soft bone on completion of the decalcification process, so as to preserve the fracture morphology. Serial sections of 6 µm thickness were cut in the coronal plane (i.e. perpendicular to the axis of the pinholes). Six coronal sections of each

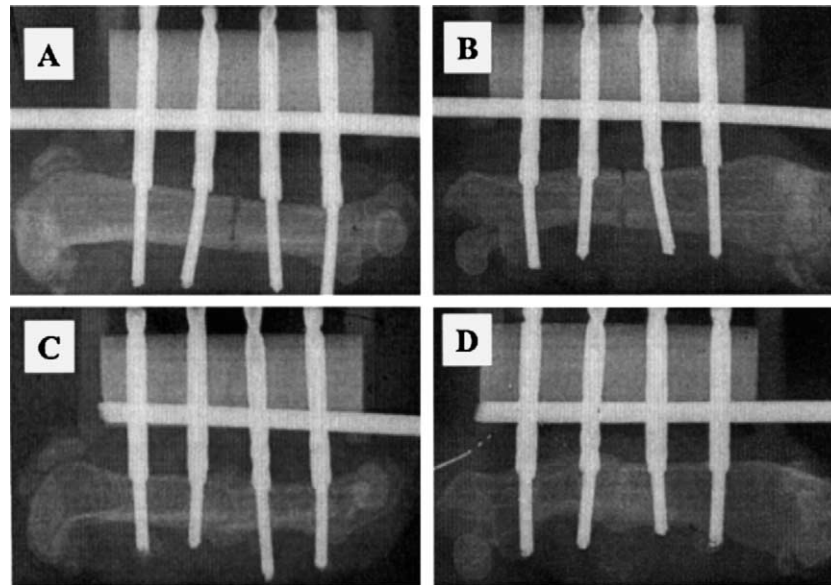


Fig. 2. Showing (A) and (C) orthogonal lateral and (B) and (D) medial oblique radiographs (A and B are of a day 4 sample and (C) and (D) of a day 24 sample). The long horizontal pin is the cross pin component of the X-ray jig.

specimen were selected at equal intervals and stained with Haematoxylin, Eosin and Alcian Blue.

All specimens were coded and analysed blindly. Light microscopy images at $50\times$ magnification were grabbed onto a Kontron Vidas Image Analyser (Kontron KMBH, Munich, Germany). The mean femoral diameter, medial, intramedullary and lateral areas of woven bone, cartilage and mesenchymal tissue were calculated in pixels, employing Scion Image Software (Scion Corporation, Maryland, USA), permitting intramedullary and peripheral areas and constituent proportions to be calculated. Measurements were performed manually by tracing around the respective areas on screen with a mouse. All areas were normalised against the mean femoral diameter on the section, also measured in pixels, in order to take account of the range of animal sizes. Therefore all areas are represented as ratios.

Mechanical testing

Nineteen of the specimens from animals sacrificed on day 16 underwent mechanical testing. After excision of the thigh and removal of the soft tissues, the external fixator was removed, employing a diamond-cutting disc (Dremmel, Hamburg, Germany) to cut the pins deep to the crossbar and a haemostat to prevent pin spinning. The pin remnants were removed by gentle anticlockwise rotation. The healing femurs were placed in labelled containers, humidified by saline-moistened gauze in the base.

Mechanical testing was performed on the same day as sacrifice. Each end of the stripped femur was mounted in self-curing orthodontic resin (Orthoresin, Dentsply, England, UK) along the central axis of DePuy CMW 2000 (DePuy, England, UK) bone cement pots. These pots were fitted to a torsional testing jig and subsequently into a test apparatus. The jig armatures produced a rotational speed of $0.143^\circ/\text{s}$ with the torsional force being transmitted to a power cell transducer (Minimat miniature materials tester, model PL2220L) via the mounted femur. The data produced was processed employing Firmware Version 3.1 (Rheometric Scientific, USA). From this a graph was generated for each specimen that enabled the peak torque (Nmm), torsional stiffness (kNmm^2/rad), and energy to peak torque or failure (Nrad) to be calculated.

Statistical analysis

All data were transferred to a statistical spreadsheet (SPSS, Version 9, Chicago, Illinois). Non-parametric methods were used: boxplots and

Mann–Whitney U tests to analyse differences between groups and Spearman rank correlation to analyse correlation between variables.

Results

Seven mice were sacrificed on day 4, 12 on day 8, 26 on day 16 and seven on day 24. There are more animals in the day 16 group, as 7 specimens underwent histomorphometry examination and 19 specimens underwent torsional testing at this time point. There were no significant differences between the groups sacrificed at the four different time points with regard to animal weights (means \pm S.D., of 41.86 ± 1.75 , 40.53 ± 2.79 , 41.98 ± 3.68 , and 39.00 ± 3.1 g respectively). The alignment of the bone fragments on X-ray was measured, the mean angulation between the fragments on the medial-oblique views was 6.8° (S.D. 5.56° , $n = 33$) for recurvatum and 1.8° (S.D. 3.52° , $n = 33$) for varus on the lateral-oblique views. No statistical difference was found between the fragment angulations on either view between time points. There were no instances of peri-pin fracture or fragment contact of less than 75% in the 52 cases; therefore all were included in the analysis.

Motion analysis

Motion analysis shows a sharp drop in the animals' motion on day one post-surgery with a gradual increase towards the pre-operative levels by day 24 as shown on Fig. 3A. There was a significant correlation between pre-operative and mean post-operative movement levels in the same mice (Spearman, $p = 0.006$, $R = 0.88$).

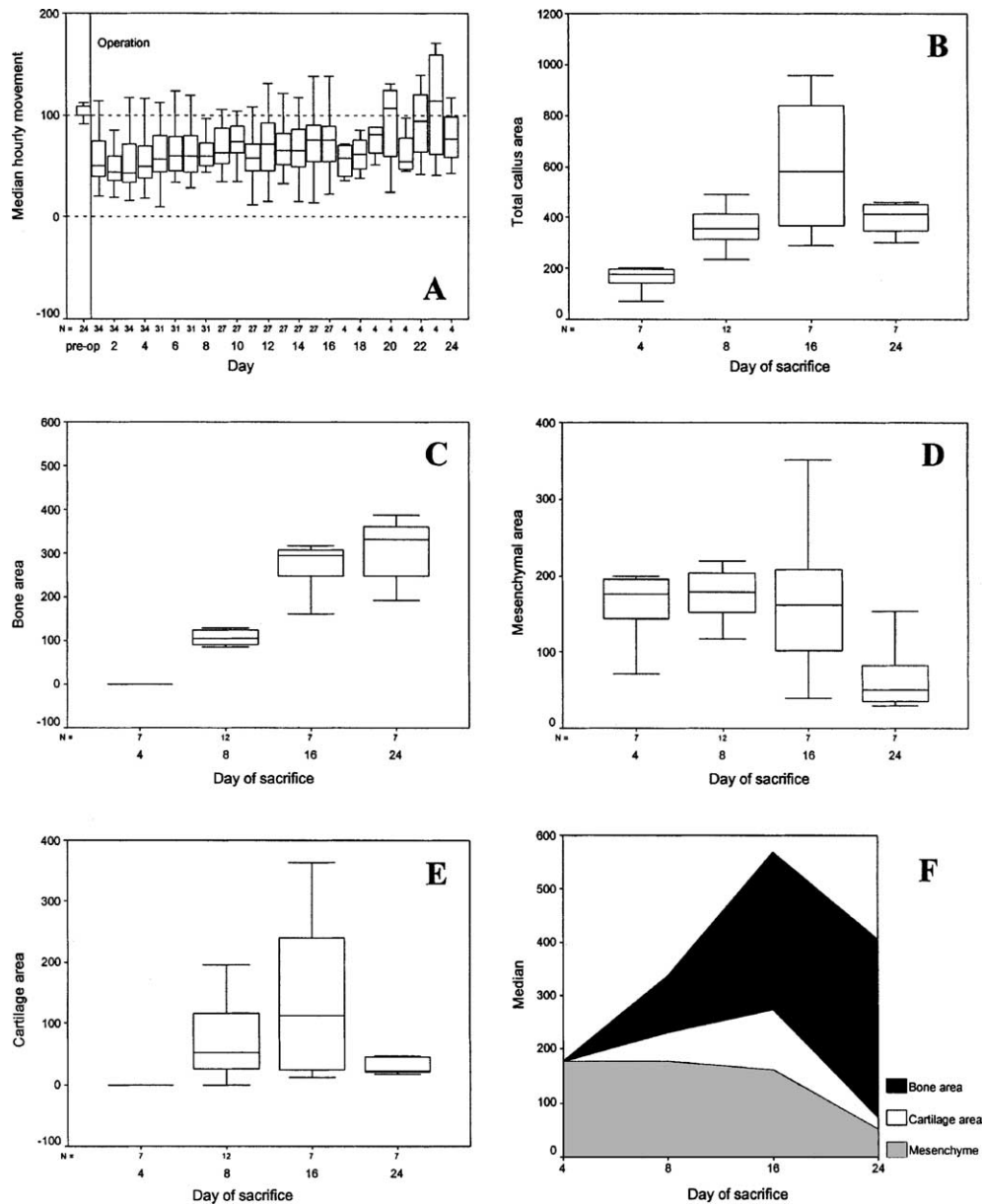


Fig. 3. (A) Comparison of the pre-operative movement against the mean movement on each post-operative day; boxplots showing (B) the increase in total callus area to day 16 and subsequent decrease, (C) the increase in new bone area, (D) the decrease in mesenchymal tissue area, (E) the increase in cartilage area to day 16 and (F) an area plot showing the callus constituents at respective time points.

Histomorphometry

Fig. 4 shows typical histological appearances from each time point. No new bone formation was evident at day 4 with the majority of bone production to day 8 being primary periosteal bone followed by endochondral ossification at day 16 and 24. Histomorphometric analysis of 33 specimens demonstrated that the total callus area increased to a maximum at day 16 and subsequently reduced (Fig. 3B). The amount of new bone increased to day 24 representing a marked rise in the proportion of the total callus area composed of new bone (Fig. 3C and F). A fall in mesenchymal area, which

constituted the total callus area at day 4 and almost none by day 24 (Fig. 3D and F), mirrored the increase in bone area. Cartilage area rose to day 16, at which point, as with the mesenchymal tissue the greatest variability was seen (Fig. 3E). After day 16 the amount of cartilage fell sharply. The inter-relationships between the constituent components of the fracture callus at each time point are summarised in Fig. 3F. The Mann–Whitney *U* test demonstrated statistical significance ($p < 0.05$) between the following healing intervals: total callus areas and bone areas between days 4, 8 and 16; cartilage area between days 4 and 8 as well as days 16 and 24; mesenchyme area between days 16 and 24.

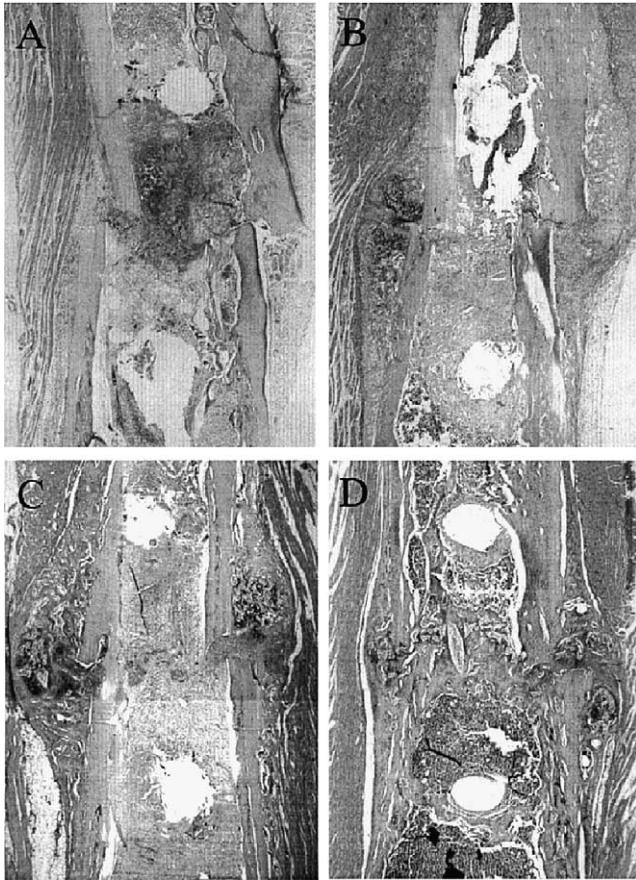


Fig. 4. Histology of fracture site at (A) day 4, (B) day 8, (C) day 16 and (D) day 24 post-fracture. The intramedullary circular deficiencies proximal and distal to the fracture are due to the external fixator pin removal prior to sectioning.

The effect of animal motion on the histomorphometric parameters

The relationship between mean hourly post-operative animal movement and the constituents of the callus was explored by non-parametric correlation. Since remodelling had started by day 24 (Fig. 4D), with callus, cartilage and mesenchymal areas falling, this was done on the specimens obtained from animals sacrificed on day 8 and 16. At these time points, the peripheral callus area, as well as the proportion of cartilage within it, increased with greater movement (Spearman, $p = 0.047$, Fig. 5).

Mechanical testing

In the day 16 mechanically tested mice, the mean peak torque, torsional stiffness and energy to failure were 11.8 Nmm (SD 11.8); 0.7 kNmm²/rad (S.D. 0.18); and 0.2 Nrad (S.D. 0.11) ($n = 19$ for all), respectively. There was a significant negative correlation between mean post-operative hourly movement and peak torque (Spearman, $p = 0.009$) and torsional stiffness ($p = 0.001$) (Fig. 6A

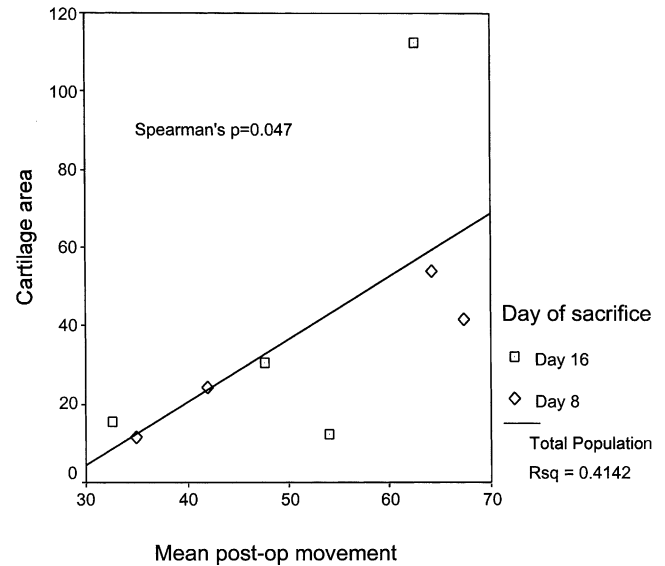


Fig. 5. Scatter plots demonstrating the correlation between day 8 and 16 cartilage areas to mean hourly post-operative animal movement (Spearman's $p = 0.047$).

and B, respectively) indicating that mice that moved more post-operatively had less well-healed fractures.

Discussion

Is this a reliable model? From a surgical point of view, the answer is yes: in this group of animals, no instances of pin failure or loss of fixation were seen and the areas of contact and alignment of the fracture fragments were consistent. Biologically, the rate of fracture healing was shown to be reproducible. For the key histomorphometric variables of total callus area and bone area, statistically significant differences were demonstrated between animals sacrificed at different time-points in keeping with the graphical representation shown in Fig. 3B and C.

In terms of the model's validity, the histological pattern of fracture repair in this model, as shown in Fig. 4, is of indirect healing with a mixture of intramembranous and endochondral ossification. This type of repair is what one would expect under the biomechanical conditions provided by the external fixation system employed. Furthermore, the modulation of healing by the mechanical environment also fits with what is known from previous work [3,6,13,18] that demonstrated variation in the parameters of indirect healing induced by variation in the mechanical properties of external fixators.

The unusual feature of this model, however, is that variation in the mechanical environment was produced by natural variation in animal behaviour, rather than by altering the fixation. The fact that between-mouse

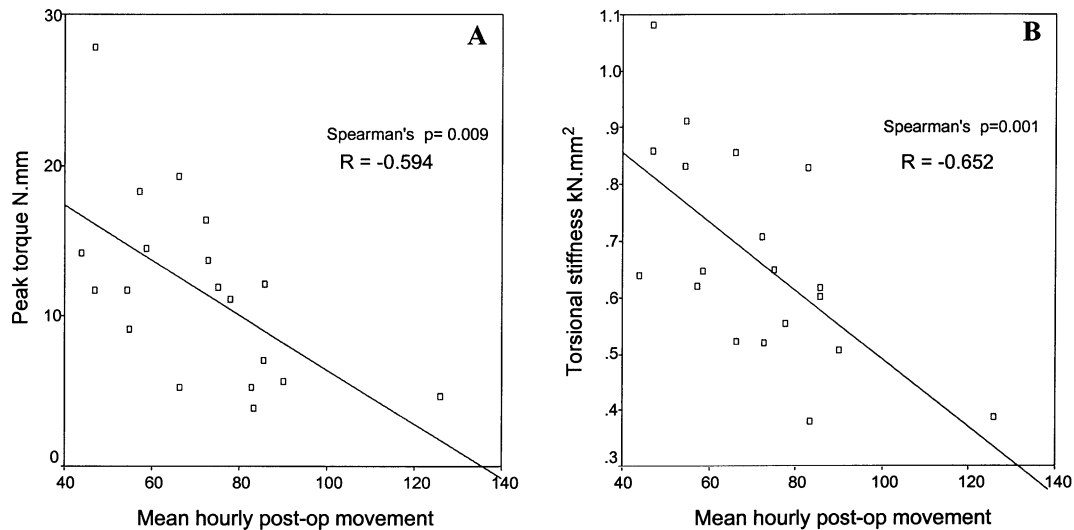


Fig. 6. Scatter plots showing (A) the negative correlation between the peak torque and (B) the torsional stiffness of day 16 healing fractures and the mean hourly post-operative movement.

variation existed pre-operatively, with mice that moved less then continuing to do so post-operatively, suggests that this is a natural phenomenon, individual to each mouse, and not due to variations in the progress of fracture healing. This is likely to be the case in other murine studies, but is usually unaccounted for. Given the marked effects of variation in movement, particularly on cartilage formation (Fig. 5) and the progress of healing as measured mechanically (Fig. 6), this is a serious omission.

The results of the present study concur with previous findings that the callus size is proportionate to the degree of interfragmentary motion [12,19,23]. Augat et al [2] showed in an externally fixated ovine model that delayed weight-bearing or decreased micromotion increased the percentage of bone in the callus whereas the amount of cartilage was increased by early weight bearing or increased micromotion. Wolf et al. [21] reported that the area of callus was significantly greater with increasing interfragmentary motion; however the greatest biomechanical stability and bone mineral density were demonstrated in callus that had undergone lower interfragmentary motion. Claes et al. [7] demonstrated, in a sheep osteotomy model, that increasing interfragmentary motion stimulated callus formation but not tissue quality. Larger strains led to mesenchymal tissue formation. Combining this data with finite element model analysis it was hypothesised that the magnitude of local stress and strain along bony surfaces predict the course and type of fracture healing [8]. Our results are also in accordance with those of Gurry et al. [10] who, using the same model, aimed to vary interfragmentary motion by varying the stiffness of the fixator. They found that a less stiff fixator led to slower healing and a larger, more cartilaginous callus.

Direct measurement of interfragmentary motion in a mouse femur is not a practical proposition. However, this movement sensor set up is feasible and relatively inexpensive. Given that we have not measured interfragmentary motion directly in this model, we cannot conclusively prove that the observed correlation between a high degree of whole-animal motion and slow healing is due to excessive interfragmentary motion at the osteotomy site. However, such a conclusion would be consistent with the data and no plausible alternative explanation springs to mind. Having standardised the mechanics of the fracture-fixator construct to the best of our ability, what we estimated, by measuring animal motion, was the number of cycles of strain, or the dose of strain, per day. The strength of the correlation between animal motion and healing would suggest that this approach is correct.

In studies using a model such as this, where test and control groups are being compared, one could of course rely on randomisation to distribute behavioural differences evenly between groups. However, this would be to lose the opportunity to understand the interaction between experimental manipulations and the mechanical environment of the fracture, as spontaneously varied by animal behaviour.

Acknowledgements

This work was funded by research grants from the Action Research, UK (grant A/P/0716) to CKC and GRD; British Orthopaedic Association Wishbone Trust grant (1999) to CKC and DRM; The R&D Office, Department of Health and Social Services, Northern Ireland (EAT/1171/99) to JRB, GL and DRM.

References

- [1] Ashurst DE. The influence of mechanical conditions on the healing of experimental fractures in the rabbit: a microscopical study. *Philos Trans R Soc London* 1986;313:271–302.
- [2] Augat P, Merk J, Ignatius A, Margevicius K, Bauer G, Rosenbaum D, et al. Early, full weight bearing with flexible fixation delays fracture healing. *Clin Orthop* 1996;328:194–202.
- [3] Bastiani D, Aldegheri R, Renzi B. Dynamic axial fixation. A rational alternative for the external fixation of fractures. *Int Orthop* 1986;10:95–9.
- [4] Bonnarens F, Einhorn TA. Short communication: production of a standard closed fracture in laboratory animal bone. *J Orthop Res* 1984;2:97–101.
- [5] Claes L, Wilke HJ, Augat P, Suger G, Fleischmann W. The influence of fracture gap, size and stability on bone healing. *Orthop Trans* 1994;18(2):425–6.
- [6] Claes LE. Mechanical enhancement of callus healing. *Clin Orthop* 1998;355:S356.
- [7] Claes LE, Heigele CA, Neidlinger W, Kaspar D, Seidl W, Margevicius KJ, et al. Effects of mechanical factors on the fracture healing process. *Clin Orthop* 1998;355:S132–47.
- [8] Claes LE, Heigele CA. Magnitudes of local stress and strain along bony surfaces predict the course and type of fracture healing. *J Biomech* 1999;32:255–66.
- [9] Greiff J. A method for the production of an undisplaced reproducible tibial fracture in the rat. *Injury* 1978;9:278–81.
- [10] Gurry J, Gregory J, Oswald B, Andrew JG. An externally fixated fracture model for the mouse femur: an in vivo study. In: *Proceedings of the British Orthopaedic Research Society, section of bioengineering, Royal Academy of Medicine in Ireland*; 1998. p. 29.
- [11] Hiltunen A, Vuorio E, Aro HT. A standardized experimental fracture in the mouse tibia. *J Orthop Res* 1993;11:305–12.
- [12] Kenwright J, Goodship AE. Controlled mechanical stimulation in the treatment of tibial fractures. *Clin Orthop* 1989;241:36–47.
- [13] Kershaw CJ, Cunningham JL, Kenwright J. Tibial external fixation, weight bearing, and fracture movement. *Clin Orthop* 1993;293:28–36.
- [14] Li G, White G, Connolly C, Marsh D. Cell proliferation and apoptosis during fracture healing. *J Bone Min Res* 2002;17:791–9.
- [15] Metsaranta M, Toman D, de Crombrughe B, Vuorio E. Specific hybridization probes for mouse type I, II, III and IX collagen mRNAs. *Biochem Biophys Acta* 1991;1089:241–3.
- [16] Molster A, Gjerdet NR, Raugstad TS, Hvidsten K, Alho A, Bang G. Effect of instability of experimental fracture healing. *Acta Orthop Scand* 1982;53:521–6.
- [17] Olmedo ML, Weiss APC. An experimental rat model allowing controlled delivery of substances to evaluate fracture healing. *J Orthop Trauma* 1994;8(6):490–3.
- [18] Park SH, O'Connor K, McKellop H, Sarmiento A. The influence of active shear or compressive motion on fracture-healing. *J Bone Jnt Surg Am* 1998;80:868–78.
- [19] Rahn B. Bone healing: histological and physiological concepts. In: Sumner-Smith G, editor. *Bone in clinical orthopaedics A study in comparative osteology*. Philadelphia: WB Saunders Company; 1982. p. 335–86.
- [20] Welch RD, Jones AL, Bucholz RW, Reinert CM, Tjia JS, Pierce WA, et al. Effect of recombinant human bone morphogenetic protein-2 on fracture healing in a goat tibial fracture model. *J Bone Miner Res* 1998;3:1483–90.
- [21] Wolf S, Janousek J, Veith F, Haas G, Claes L. The effect of external mechanical stimulation on the healing of diaphyseal osteotomies fixed by flexible external fixation. *Clin Biomech* 2001;13:359–64.
- [22] Wu J, Shyr HS, Chao EYS, Kelly PJ. Comparison of osteotomy healing under external fixation devices with different stiffness characteristics. *J Bone Jnt Surg Am* 1984;66:1258–64.
- [23] Yamagishi M, Yoshimura Y. The biomechanics of fracture healing. *J Bone Jnt Surg Am* 1955;37:1035–68.